Published in final edited form as:
Chem Biol. 2011 October 28; 18(10): 1300–1311. doi:10.1016/j.chembiol.2011.07.020.

Disruption of Wnt Planar Cell Polarity Signaling by Aberrant Accumulation of the MetAP-2 Substrate Rab37

Thomas B. Sundberg[1], **Nicole Darricarrere**[2], **Pasquale Cirone**[1], **Xia Li**[1], **Lucy McDonald**[3], **Xue Mei**[4], **Christopher J. Westlake**[5], **Diane C. Slusarski**[4], **Robert J. Beynon**[3], and **Craig M. Crews**[1,6,7,*]

[1]Department of Molecular, Cellular, and Developmental Biology, Yale University, New Haven, CT 06511, USA

[2]Department of Cell Biology, Yale University, New Haven, CT 06511, USA

[3]Protein Function Group, Institute of Integrative Biology, University of Liverpool, Crown Street, Liverpool L69 7ZB, UK

[4]Department of Biology, University of Iowa, Iowa City, IA 52242, USA

[5]Genentech, South San Francisco, CA 94080, USA

[6]Department of Pharmacology, Yale University, New Haven, CT 06511, USA

[7]Department of Chemistry, Yale University, New Haven, CT 06511, USA

SUMMARY

Identification of methione aminopeptidase-2 (MetAP-2) as the molecular target of the antiangiogenic compound TNP-470 has sparked interest in N-terminal Met excision's (NME) role in endothelial cell biology. In this regard, we recently demonstrated that MetAP-2 inhibition suppresses Wnt planar cell polarity (PCP) signaling and that endothelial cells depend on this pathway for normal function. Despite this advance, the substrate(s) whose activity is altered upon MetAP-2 inhibition, resulting in loss of Wnt PCP signaling, is not known. Here, we identify the small G-protein Rab37 as a novel MetAP-2 substrate that accumulates in the presence of TNP-470. A functional role for aberrant Rab37 accumulation in TNP-470's mode-of-action is demonstrated using a Rab37 point-mutant that is resistant to NME because expression of this mutant phenocopies the effects of MetAP-2 inhibition on Wnt PCP signaling-dependent processes.

INTRODUCTION

Angiogenesis is the process of forming new blood vessel from the existing vasculature and is essential for normal development (Carmeliet, 2005). However, because inappropriate blood vessel formation contributes to many disease processes including rheumatoid arthritis, endometriosis, diabetic retinopathy, macular degeneration and tumorigenesis, antiangiogenic therapy has broad clinical potential (Folkman, 2007). The microbial metabolite fumagillin

*Contact: Craig Crews; craig.crews@yale.edu; (tel) 203-432-9364; (fax) 203-432-6161.

CONFLICTS OF INTEREST

The authors declare no conflict of interest.

and its synthetic derivatives (e.g., TNP-470) are potent, first-in-class small molecule angiogenesis inhibitors with established efficacy *in vivo* (Ingber, et al., 1990; Kruger and Figg, 2000). Affinity chromatography with biotinylated fumagillin derivatives identified the metalloprotease methionine aminopeptidase-2 (MetAP-2), one of two proteins responsible for N-terminal methionine excision (NME) in eukaryotes, as the molecular target responsible for fumagillin/TNP-470's antiangiogenic activity (Griffith, et al., 1997; Sin, et al., 1997; Yeh, et al., 2006). This discovery has stimulated interest in the exquisite sensitivity of endothelial cells to loss of MetAP-2 activity, relative to non-endothelial cell-types and inspired development of several novel structural classes of MetAP-2 inhibitors (Arico-Muendel, et al., 2009; Marino, et al., 2007; Wang, et al., 2007; Wang, et al., 2008).

Recently, our lab demonstrated that MetAP-2 inhibition suppresses Wnt planar cell polarity (PCP) signaling (Zhang, et al., 2006), an intracellular signaling network activated by binding of secreted Wnt proteins to Frizzled (Fz) seven-pass transmembrane receptors (Angers and Moon, 2009). Wnt-Fz complexes transduce signaling through the intracellular scaffolding protein Dishevelled (Dvl) leading to activation of various downstream effectors (Angers and Moon, 2009). MetAP-2 inhibition specifically suppresses activation of downstream effectors Wnt PCP signaling such as c-Jun N-terminal kinase and the small G-protein RhoA (Zhang, et al., 2006). We, and others, have also demonstrated that normal endothelial cell function depends on finely balanced Wnt PCP signaling; expressing a dominant-negative Dishevelled mutant, knockdown of *wnt5* or expression of a constitutively active form of the Wnt PCP effector DAAM1 suppress endothelial cell proliferation and impairs angiogenesis *in vivo* (Cheng, et al., 2008; Cirone, et al., 2008; Ju, et al., 2010; Masckauchan, et al., 2006).

Although several preferential MetAP-2 substrates (e.g., GAPDH, cyclophillin A and thioredoxin-1) have been identified, N-terminal Met retention on these proteins does not contribute to the effects of MetAP-2 inhibition on Wnt PCP signaling and angiogenesis (Wang, et al., 2008; Warder, et al., 2008). Here, using an unbiased N-terminal positional proteomics screen, we identify Rab37 as a preferential MetAP-2 substrate that aberrantly accumulates in the presence of TNP-470 and, when overexpressed, phenocopies the effects of MetAP-2 inhibition on Wnt PCP signaling-dependent processes such as endothelial cell proliferation/network formation and zebrafish embryogenesis.

RESULTS

Identification of Preferential MetAP-2 Substrates by N-terminal Proteomics

Given that methionine aminopeptidases are responsible for NME, we reasoned that an N-terminal positional proteomics screen would be well suited for identification of proteins that retain their N-terminal Met residue following MetAP-2 inhibition. Our N-terminal positional proteomics approach (see Figure 1), generates an enriched pool of N-terminal peptides that can more easily be identified by liquid chromatography-tandem mass spectroscopy (LC-MS/MS) than global proteomic preparations (McDonald, et al., 2005).

For this study, murine pulmonary endothelial (MPE) cells were cultured in media containing stable heavy isotope-labeled arginine ($[^{13}C_6]$Arg) for seven passages before exposure to TNP-470 (50 nM, 16 hr). A control set of MPE cells were maintained in unlabelled media and then treated with vehicle. Following cell lysis, soluble fractions from the two treatment conditions were pooled and used to generate N-terminal peptide preparations. While stable isotope-labeled ('heavy') N-terminal peptides are derived from TNP-470-treated cells, the unlabeled ('light') counterparts from vehicle-treated cells should show normal processing. In this experiment, essentially all of the identified N-terminal peptides produced LC-MS/MS signals of equivalent intensity suggesting that MetAP-2 is redundant for NME for most proteins. In contrast, abundance of the heavy (TNP-470-treated) versus light (vehicle-

treated) N-terminal peptide corresponding to glyceraldehyde 3-phosphate dehydrogenase (GAPDH) was elevated approximately three-fold (Figure 2A). This data is consistent with previous reports indicating that GAPDH is preferentially processed by MetAP-2 (Turk, et al., 1999; Wang, et al., 2008), and suggests N-terminal positional proteomics is a viable approach to identify novel MetAP-2 substrates.

Rab37 is a Novel MetAP-2 Substrate

In addition to GAPDH, another protein that displayed an isotope-labeling pattern consistent with MetAP-2 processing was the low-molecular-weight G-protein Rab37 (Figure 2B). In fact, unlabelled N-terminal peptide was not detected in this case suggesting that Rab37 is destabilized by NME, and thus, accumulates in the presence of TNP-470. As a first step, we sought to independently confirm this result by determining if Rab37 accumulates upon MetAP-2 inhibition. Because available antibodies were unable to detect either endogenous or ectopically expressed Rab37, we transiently transfected human embryonic kidney (HEK) 293T cells with a Rab37 construct containing a FLAG epitope tag beginning at N+3 position (WT-Rab37) thereby preserving the endogenous N-terminus of Rab37 (Figure 2C). In vehicle-treated cells, WT-Rab37 was present at low levels, whereas inhibition of MetAP-2 with TNP-470 led to a large (>10-fold) increase in Rab37 abundance (Figure 2D). To determine if TNP-470-induced Rab37 accumulation is directly related to N-terminal Met retention, we transiently expressed equivalent amounts of WT-Rab37 (50 ng) or a mutant (T2E-Rab37) that is completely resistant to MetAP-2 processing due to substitution of the penultimate N-terminal Thr to Glu (Xiao, et al., 2010). Basal levels of this MetAP-2-resistant mutant are >10-fold higher than WT-Rab37, and did not further increase in the presence of TNP-470 (Figure 2D). Importantly, abundance of T2E-Rab37 was essentially equivalent to that of WT-Rab37 in TNP-470-treated cells (Figure 2D), suggesting that T2E-Rab37 is stabilized relative to the wildtype protein due to inhibition of NME. These data, along with the results of our N-terminal proteomic study, indicate that Rab37 is a novel MetAP-2 substrate that is destabilized by NME, and thus, accumulates in the presence of TNP-470.

Subcellular Localization of Rab37 in Endothelial Cells

Rab GTPases are members of the Ras superfamily of low-molecular-weight G-proteins that function as key regulators of intracellular trafficking in eukaryotic cells (for reviews, see (Pfeffer and Aivazian, 2004; Stenmark, 2009)). The >60 Rab proteins in metazoan cells are localized to specific organelles where they regulate vesicular transport by recruiting effectors such as lipid kinases/phosphatases, motor proteins and membrane tethering factors (Grosshans, et al., 2006). Rab37 has been reported to associate with secretory granules in mast cells and pancreatic β-cells (Brunner, et al., 2007; Masuda, et al., 2000), leading to the assumption that it plays a role in exocytosis (Stenmark, 2009). However, Rab37 was recently identified in a proteomic analysis of the endoplasmic reticulum-Golgi intermediate compartment of hepatocarcinoma cells (Breuza, et al., 2004). Given these conflicting results, we sought to define the subcellular localization of Rab37 in endothelial cells by transiently expressing WT-Rab37 in human umbilical vein endothelial (HUVE) cells. In these cells, WT-Rab37 displayed a peri-nuclear, crescent-shaped distribution suggestive of localization to the Golgi, which is further supported by colocalization with the Golgi marker Giantin (Figure 3A). Transiently expressed T2E-Rab37 was detected more readily than wildtype protein (i.e., photodetector sensitivity was increased for WT-Rab37 relative to T2E-Rab37 to obtain similar intensity staining), and was also localized to a peri-nuclear compartment closely associated with the Golgi resident protein Giantin (Figure 3A). Thus, unlike abundance, localization of Rab37 to the Golgi is not affected by N-terminal Met retention.

To determine if transient expression of any Rab protein in endothelial cells is sufficient to induce accumulation in the Golgi, HUVE cells were co-transfected with WT-Rab37 and RFP-Rab5, a Rab protein associated with early endosomes (Bucci, et al., 1992). While RFP-Rab5 displayed cytosolic, vesicular staining consistent with localization to early endosomes, Rab37 was again detected in peri-nuclear clusters (Figure S1). In addition, wildtype Rab37 bearing an N-terminal GFP co-localized with the Golgi resident protein GM130 when expressed in MPE cells (Figure S2), which indicates that Rab37 is localized to the Golgi in endothelial cells derived from different species and anatomical origins.

Trafficking of Rab proteins from loading to docking membranes is associated with a transition from GDP to GTP binding (Stenmark, 2009). Because the catalytic site of Rab proteins is highly conserved, well-characterized mutants can be prepared in which the GTP (Q89L for Rab37)- or GDP (T43N for Rab37)-bound state is stabilized (Masuda, et al., 2000). Determining the subcellular localization of these GTPase cycle mutants can provide clues about the intracellular trafficking processes regulated by a particular Rab protein (Stenmark, 2009). Expression of Rab37-T43N could not be detected in transiently transfected HUVE or MPE cells preventing analysis of the subcellular distribution of Rab37 GTPase cycle mutants in endothelial cells. In HEK 293T cells, WT-Rab37 and the GTP stabilized mutant are primarily detected in a peri-nuclear compartment that co-localizes with the Golgi marker Giantin (Figure 3B), and display little overlap with other organelles involved in intracellular vesicular trafficking such as the endoplasmic reticulum (Figure S3). In contrast, a significant portion of Rab37-T43N staining was detected at the plasma membrane in this cell type (Figure 3B). These data indicate that wildtype Rab37 is localized to the Golgi in both endothelial and non-endothelial cell types where it is likely to play a role in retrograde transport from the plasma membrane.

Aberrant Rab37 Accumulation Selectively Disrupts Endothelial Cell Function

Given that Rab37 levels increase in the presence of TNP-470, it is intriguing that a number of Rab proteins or their effectors have been shown to regulate Wnt PCP signaling (Lee, et al., 2007; Mottola, et al., 2010; Pataki, et al., 2010; Purvanov, et al., 2010). Thus we hypothesized that aberrant accumulation of Rab37 following inhibition of MetAP-2 may act via a ‘gain-of-function’ mechanism to disrupt Wnt PCP signaling, and as a result, endothelial cell homeostasis. We evaluated this model by comparing the effects of stably expressing WT- or T2E-Rab37 in HEK 293T versus HUVE cells to determine if accumulation of Rab37 ‘phenocopies’ the endothelial cell-selective antiproliferative activity of MetAP-2 inhibition. HEK 293T and HUVE lines stably expressing WT- or T2E-Rab37 or a GFP control were generated by infection with retroviral expression constructs followed by puromycin selection. T2E-Rab37 was observed at ≈3-fold higher levels than wildtype protein in both HUVE and HEK 293T cells (Figure 4A). These data are consistent with transient expression in HEK 293T cells (Figure 2D), and suggest that N-terminal Met retention also promotes aberrant Rab37 accumulation in endothelial cells.

Stable expression of WT- or T2E-Rab37 did not significantly alter the proliferative capacity of HEK 293T cells (Figure 4B). Although HUVE cells stably expressing WT-Rab37 displayed a modest (≈15%) decrease in [^{3}H]-thymidine incorporation, this effect did not achieve statistical significance. In contrast, stable expression of T2E-Rab37 results in an approximately 50% reduction in proliferative capacity (Figure 4B), a change that was not associated with increased cell death as measured by vital dye exclusion (data not shown). To examine whether the growth inhibitory effect of T2E-Rab37 expression in HUVE cells results from locating the FLAG epitope tag near the N-terminus, we prepared untagged wildtype Rab37 and the T2E mutant as well as constructs containing a FLAG epitope tag 16 residues proximal to the C-terminus, which is not predicted to disrupt the C-terminal prenylation motif (Figure S4A). These constructs were stably expressed in HUVE cells via

retroviral infection/puromycin selection (Figure S4B). Consistent with N-terminal FLAG epitope-tagged Rab37, expression of wildtype untagged or C-terminal tagged Rab37 did not alter the proliferative capacity of HUVE cells (Figure S4C). In contrast, [^{3}H]-thymidine incorporation was reduced by nearly 50% and 30% in HUVE cells expressing the untagged or C-terminal tagged T2E-Rab37, respectively, relative to GFP control cells (Figure S4C). Along with reduced basal proliferative capacity, HUVE cells stably expressing T2E-Rab37 were approximately three-fold more sensitive to TNP-470-induced growth arrest than control cells expressing GFP with EC_{50} values of 60 ± 10 versus 180 ± 20 pM, respectively (Figure 4C). In contrast, expression WT-Rab37 did not affect the EC_{50} for TNP-470-induced growth arrest in HUVE cells (Figure 4C). Together, the ability of T2E-Rab37 to selectively suppress endothelial cell proliferation and to sensitize HUVE cells to TNP-470 supports a model in which N-terminal Met retention on Rab37 contributes to growth arrest following MetAP-2 inhibition.

In vivo, angiogenesis involves migration and intercellular communication between endothelial cells in addition to proliferation (Carmeliet, 2005). Hence, the antiangiogenic effects of MetAP-2 inhibition suggest that aberrant Rab37 accumulation might also perturb these processes. Organization of endothelial cells into coordinated tubular networks when cultured on Matrigel™ basement membrane is a quantitative *in vitro* proxy of angiogenesis (Staton, et al., 2004). As shown in Figure 4D, HUVE cells stably expressing GFP formed similar numbers of cell extensions as a mock infected control (108 ± 10 versus 89 ± 8 extensions/field-of-view, respectively), which indicates that retroviral infection/puromycin selection does not impair this process. By contrast, HUVE cells stably expressing WT- or T2E-Rab37 formed 36 ± 6 or 15 ± 4 extensions/field-of-view, respectively, which corresponds to a 60 or 85% decrease relative to GFP control (Figure 4D). Because endothelial cell network formation correlates with angiogenic potential (Staton, et al., 2004), these data suggest that aberrant accumulation of Rab37 plays a role in the antiangiogenic effects of MetAP-2 inhibition.

Activation of Wnt PCP Signaling Suppresses Rab37-Induced Growth Arrest

Given that expression of T2E-Rab37 phenocopies the inhibitory effects of fumagillin/TNP-470 on Wnt PCP signaling-dependent processes in endothelial cells, we next explored whether Rab37-induced growth arrest could be rescued by constitutive activation of this signaling cascade. To address this question, HUVE cells stably expressing a Dvl2 deletion mutant (ΔDIX-Dvl2) or the corresponding empty vector were generated by retroviral infection followed by zeocin selection (Figure 4E). Deletion of the Dishevelled amino-terminal DIX domain results in selective activation of Wnt PCP signaling in a Fz-independent manner (Heisenberg, et al., 2000; Tada and Smith, 2000; Wallingford and Habas, 2005), and expression of ΔDIX-Dvl2 rescues endothelial cells from TNP-470-induced growth arrest (Zhang, et al., 2006). Next, HUVE cells expressing ΔDIX-Dvl2 or the corresponding empty vector were infected with retroviruses encoding GFP or T2E-Rab37 and stable integrants selected with puromycin (Figure 4E). Similar to Figure 4B, expression of T2E-Rab37 reduced [^{3}H]-thymidine incorporation by ≈40% compared to GFP in HUVE cells first infected with empty vector (Figure 4F). While expression of ΔDIX-Dvl2 decreased [^{3}H]-thymidine incorporation by ≈50% relative to empty vector, T2E-Rab37 did not further reduce proliferative capacity of HUVE cells expressing this construct (Figure 4F). The ability of ΔDIX-Dvl2 to render HUVE cells resistant to T2E-Rab37-induced growth arrest suggests that disruption of Wnt PCP signaling contributes to the deleterious effects of aberrant Rab37 accumulation on normal endothelial cell function.

Rab37 Knockdown Selectively Suppresses Endothelial Cell Proliferation

Normal development requires finely balanced Wnt PCP signaling; both knockdown and overexpression of Wnt PCP proteins (e.g., Dishevelled) disrupts this pathway leading to abnormal phenotypes (Seifert and Mlodzik, 2007; Wallingford, et al., 2000). Given that aberrant accumulation of Rab37 suppresses Wnt PCP-dependent processes, we next asked what effect depleting Rab37 has on endothelial cell proliferation. For this experiment, Rab37 expression was stably reduced in HUVE cells by infection with two separate lentiviral shRNA constructs targeting Rab37 or a non-targeting scramble shRNA construct followed by puromycin selection. Because endogenous Rab37 could not be detected in HUVE cells, we simultaneously infected a HEK 293 clone stably expressing WT-Rab37, which resulted in a >90% decrease in Rab37 protein levels relative to the non-targeting scramble shRNA (Figure 5A). Although near-complete knockdown of Rab37 modestly inhibited proliferation of HEK 293 cells measured in terms [^{3}H]-thymidine incorporation (Figure 5B), this trend failed to achieve statistical significance. In contrast, stable knockdown of Rab37 in HUVE cells decreased [^{3}H]-thymidine incorporation >75% relative to the scramble shRNA control (Figure 5B). Levels of [^{3}H]-thymidine incorporation in HUVE cells expressing the shRNA scramble sequence are reproducibly ≈2-fold higher than those stably infected with GFP (Figure 5C versus Figure 4C and 4E), a decrease likely attributable to differential effects of lenti- versus retroviral infection, respectively. Although growth arrest induced by Rab37 depletion in HUVE cells substantially obscures the antiproliferative effects of MetAP-2 inhibition, [TNP-470] ≥1 nM reduced [^{3}H]-thymidine incorporation ≈2-fold in Rab37 knockdown HUVE cells (Figure 5C). While these data suggest that N-terminal Met retention on additional MetAP-2 substrates may contribute to growth arrest induced by fumagillin/TNP-470, the endothelial cell-selective antiproliferative effect of Rab37 knockdown is consistent with this protein playing a previously unappreciated role in Wnt PCP signaling in this cell-type.

Effect of Rab37 Expression on Zebrafish Embryogenesis

Wnt PCP signaling plays a regulatory role in convergence-extension (CE) movements during vertebrate gastrulation (Seifert and Mlodzik, 2007). For instance, loss-of-function mutations in the *wnt5* locus lead to a characteristic truncated, kinked *pipetail* (*ppt*) morphology and accompanying vascular defects during zebrafish embryogenesis (Cirone, et al., 2008; Rauch, et al., 1997). An analogous phenotype is observed in zebrafish embryos where MetAP-2 function is reduced by TNP-470 or downregulation of *metap2* with antisense morpholino oligonucleotides (Cirone, et al., 2008; Zhang, et al., 2006). To determine if Rab37 expression phenocopies the effects of MetAP-2 inhibition on CE, zebrafish embryos were injected with equivalent amounts of RNA encoding untagged wildtype Rab37 or the MetAP-2-resistant T2E mutant. For T2E-Rab37, the injected embryos displayed a moderately penetrant (≈25% of embryos) phenotype characterized by a shortened, kinked tail reminiscent of the morphology resulting from downregulation of *wnt5* or *metap2* (Figure 6A and Table 1). Careful examination of the T2E-Rab37 injected embryos revealed formation of C-shaped somites and undulations in the notochord, which contrasts with the straight notochord and chevron-shaped somites in control embryos (Figure 6A). While similar phenotypes were observed in WT-Rab37 injected embryos, these effects were both milder and less penetrant (Figure 6A and Table 1).

To determine whether molecular evidence Wnt PCP signaling loss accompanied these morphological changes, we co-injected embryos with RNA encoding membrane-localized mCherry and Centrin-GFP in the presence or absence of T2E-Rab37. Centrin-GFP is a viable marker for basal bodies at the base of cilia projecting from neural floorplate glia (Piel, et al., 2000), and Wnt PCP signaling is implicated in polarized ciliogenesis in this organ during zebrafish embryogenesis (Borovina, et al., 2010). In control-injected embryos, neural

floorplate shows and ordered, interlaced pattern with many basal bodies docked at the posterior membrane (Figure 6B). In contrast, the morphological abnormalities in T2E-Rab37-injected embryos were accompanied by loss of neural floorplate organization and random localization of Centrin-GFP (Figure 6B), both effects that are consistent with aberrant Rab37 levels acting to compromise Wnt PCP signaling.

We previously demonstrated that perturbation of Wnt PCP signaling by *wnt5* knockdown or overexpression of the Wnt PCP effector DAAM1 leads to vascular defects during zebrafish embryogenesis (Cirone, et al., 2008; Ju, et al., 2010). Similarly, embryos injected with T2E-Rab37, but not wildtype protein, were characterized by an accumulation of blood posterior to the yolk extension, which is indicative of defective vasculogenesis (Figure 6A). The increased severity of the developmental abnormalities in T2E- versus WT-Rab37 injected embryos is consistent with our endothelial cell culture data and suggests that N-terminal Met retention promotes Rab37 accumulation and disruption of Wnt PCP signaling-dependent processes in a variety of contexts.

DISCUSSION

Owing to the subtlety of the structural change resulting from N-terminal Met retention, identification of preferential MetAP-2 substrates has proven challenging using global proteomics techniques. Here we employ a positional proteomics strategy to enrich N-terminal peptides enabling specific analysis of how MetAP-2 inhibition affects both protein abundance and N-terminal amino acid composition in endothelial cells. Despite this highly sensitive and focused approach, levels of nearly all the detected N-terminal peptides were not altered by TNP-470 treatment, which suggests that MetAP-2 specifically processes a very small subset of proteins. A more prominent role for MetAP-1 in bulk NME is consistent with the dramatic growth inhibitory effect of deleting *map1* in yeast, relative to the mild phenotype observed in *Δmap2* strains (Li and Chang, 1995). However, in this study, TNP-470 treatment led to N-terminal Met retention on Rab37 (N-terminus: Met-Thr-Gly N-terminus) as well as on the previously identified substrate GAPDH (N-terminus: Met-Val-Lys), which is consistent with recent biochemical analysis of NME indicating that proteins beginning with Met-Thr or Met-Val are preferentially processed by MetAP-2 (Xiao, et al., 2010). In accordance with previous studies, TNP-470 treatment did not significantly elevate GAPDH levels (Turk, et al., 1999; Wang, et al., 2008). In contrast, Rab37 abundance is dramatically increased by MetAP-2 inhibition, which appears to be a direct consequence of N-terminal Met retention because the MetAP-2-resistant T2E-Rab37 mutant is detected at equivalent levels as wildtype protein in the presence of TNP-470. The differential accumulation of GAPDH versus Rab37 in response to TNP-470 is likely related to the turnover rate of each protein. While the subtle effects of MetAP-2 inhibition on GAPDH abundance are consistent with the low rate of GAPDH turnover ($t_{½}$ ≈38 hr) (Franch, et al., 2001), the pronounced increase in levels of Rab37 bearing an N-terminal Met residue in TNP-470 treated endothelial cells suggests this protein is degraded/resynthesized at significantly faster rate.

A recent extension of Varshavsky's N-End-Rule indicates that acetylated N-terminal Met, Ala, Ser, Thr, Cys, and Val residues are specifically recognized by the E3 ubiquitin ligase Doa10 (Teb4 in metazoans) leading to degradation by the ubiquitin-proteasome system (Hwang, et al., 2010). Acetylation of N-terminal Met residues by the NatB complex requires the presence of charged or bulky, hydrophobic penultimate residues, which also prevent NME (Arnesen, et al., 2009). In contrast, N-terminal Ala, Ser, Thr, Cys, and Val residues revealed by NME are acetylated by the NatA complex (Arnesen, et al., 2009). Perhaps, retention of the N-terminal Met residue on Rab37 following MetAP-2 inhibition prevents acetylation by NatA, and as a result, Doa10/Teb4-mediated proteasomal degradation.

Consistent with this model, endothelial cell-specific knockout of the NatA component *NAA15*, which should suppress Rab37 N-terminal acetylation, results in vascular defects in mice (Wall, et al., 2004).

Genetic studies in model organisms such as *Drosophila* have identified 'core' PCP proteins whose asymmetric cellular localization is required for normal formation of polarized tissues across phyla (Seifert and Mlodzik, 2007). Perhaps not surprisingly given their central role in intracellular trafficking, an emerging body of evidence implicates Rab proteins in Wnt PCP signaling. For example, Rab23 loss-of-function alleles induce trichome misorientation in *Drosophila* wings and knockdown of Rab40 in *Xenopus* embryos disrupts CE movements during embryogenesis (Lee, et al., 2007; Pataki, et al., 2010). Moreover, normally functioning Wnt PCP signaling requires precisely coordinated intracellular trafficking as evidenced by the multiple wing hair phenotype observed in *Drosophila* expressing a gain-of-function, GTP-stabilized Rab11-QL allele, which disrupts Wnt PCP signaling due to unchecked recycling of Fz receptors to the plasma membrane (Purvanov, et al., 2010). These findings support a model whereby aberrant accumulation of Rab37 following MetAP-2 inhibition disrupts Wnt PCP signaling, and as a result, compromises endothelial cell function. Although expression of T2E-Rab37 selectively suppresses endothelial cell proliferation, this reduction is less pronounced than the effects on endothelial cell network formation and zebrafish embryogenesis. This difference may imply that N-terminal Met retention on additional MetAP-2 substrates contributes to the antiproliferative activity of fumagillin/TNP-470. Alternatively, the inhibitory effects of T2E-Rab37 expression on Wnt PCP signaling may be more profound in assays that better recapitulate the complex, multi-cellular processes underlying angiogenesis *in vivo*.

The subcellular distribution of the Rab37 GTPase cycle mutants suggests a role for this protein in plasma membrane to Golgi trafficking. Normal function of many core Wnt PCP signaling components (e.g., Fz and Dvl) depends on their localization to the plasma membrane (Seifert and Mlodzik, 2007). As such, it is tempting to speculate that aberrant accumulation of Rab37 might, opposite of the mechanism induced by Rab11-QL mutants, sequester Wnt PCP components in the Golgi thereby disrupting normal signaling. Regardless of the mechanism involved, the discovery and functional validation of Rab37 as a novel MetAP-2-specific substrate provides new insight in fumagillin/TNP-470's mode-of-action and identifies a previously unrecognized regulatory role for this protein in Wnt PCP signaling.

SIGNIFICANCE

The microbial metabolite fumagillin and its synthetic derivatives (e.g., TNP-470) possess promising antiangiogenic and antitumor activities derived from exquisite, cell-type selective arrest of endothelial cell proliferation. The metalloprotease methionine aminopeptidase-2 (MetAP-2), one of two proteins that mediate N-terminal Met excision, is the molecular target responsible for fumagillin/TNP-470's antiangiogenic activity. Recently, we demonstrated that MetAP-2 inhibition suppresses Wnt planar cell polarity (PCP) signaling and that disruption of this pathway impairs endothelial cell function leading to vascular defects during zebrafish embryogenesis. Despite this advance, the identity of the MetAP-2 substrate(s) whose function is altered in the presence of fumagillin/TNP-470 resulting in loss of Wnt PCP signaling has remained enigmatic. Here, we employed an N-terminal positional proteomics strategy to screen for MetAP-2-specific substrates. This unbiased approach identified Rab37 as a novel protein whose N-terminal Met-retained form is highly enriched in endothelial cells following MetAP-2 inhibition. Significantly, expression of a Rab37 point-mutant that is resistant to MetAP-2 processing phenocopies the inhibitory effects fumagillin/TNP-470 on Wnt PCP signaling-dependent processes such as endothelial

cell proliferation/network formation as well as vascularization during zebrafish embryogenesis. These findings position aberrant Rab37 accumulation as a critical component of mechanism underlying the antiangiogenic effects of MetAP-2 inhibition. Perhaps more generally, identification of Rab37 as novel regulator of Wnt PCP signaling corresponds to an emerging body of evidence implicating Rab proteins in the normal organization/function of the Wnt PCP signaling machinery. Therefore, further study of how aberrant Rab37 accumulation disrupts Wnt PCP signaling should provide fresh insight into how this signaling network regulates endothelial cell function.

EXPERIMENTAL PROCEDURES

Cell culture

Tissue culture reagents, including fetal bovine serum (FBS), were obtained from Invitrogen (Carlsbad, CA). Primary HUVE cells were obtained from the Yale University Vascular Biology & Therapeutics Program and maintained in EGM-2-MV media (Lonza, Basel, Switzerland). HEK 293T cells obtained from the American Type Culture Collection (Manassas, VA) and gp293 retroviral packing cells (BD Biosciences, Franklin Lakes, NJ) were cultured in Dulbecco's Modified Eagle Medium (DMEM) supplemented with 10% FBS (vol/vol) and penicillin (100 μg/mL) streptomycin (100 U/mL). Cells were transfected using Lipofectamine 2000 (Invitrogen) according to the manufacturer's instructions. For stable expression of WT-Rab37, pCDNA5/FRT/WT-Rab37 was co-transfected in 1:9 ratio with pOG4 (FRT plasmid) into 293 FlpIn cells (Invitrogen) followed by selection of stable clones with hygromycin B (100 μg/mL). For retroviral infections pBABE.puro/WT- or T2E-Rab37 or pBABE.ble/HA-ΔDIX-Dvl2 were co-transfected in a 1:1 ratio with pMD2.G (cat# 12259, Addgene, Cambridge, MA) into gp293 retroviral packaging cells. For stable knockdown of Rab37, HEK 293T cells were co-transfected in a 1:3:3 ratio with pMD2.G and psPAX2 (cat# 12260, Addgene) along with pLKO shRNA vectors targeting Rab37 (cat# RHS4552-NM_001006638; Open Biosystems, Huntsville, AL) or a non-targeting scramble shRNA (cat# 1864, Addgene). After 48 hr, viral supernatants were harvested, passed through a 0.45-μm filter, and added directly to the growth media of target cells that had been supplemented with polybrene (8 μg/mL). After an additional 48 hr, stable integrants were selected with puromycin (0.5 μg/mL) or zeocin (100 μg/mL). Organic compounds were dissolved in cell culture growth media containing ≤0.5% DMSO.

PCR and plasmid construction

pCMV-Sport6/hRab37 (cat# BC016615) was purchased from Open Biosystems (Huntsville, AL). Wildtype and T2E-Rab37 bearing a FLAG epitope tag at the N+3 position were generated by PCR amplification using the primer sets (FP: 5′-ATATGCGGATCCGCCACCATGACGGGCGATACAAGGATGACGACGATAAGACGCCAGGCGCCGTTGCC-3′ and RP: 5′-ATGCTATCTAGATCACATGAAGGAGCAGCAGCT-3′) or (FP: 5′-ATATGCGGATCCGCCACCATGGAAGGCGATTACAAGGATGACGACGATAAGACGCCAGGCGCCGTTGCC-3′ and RP: 5′-ATGCTATCTAGATCACATGAAGGAGCAGCAGCT-3′), respectively, and cloned into the *Bam*HI/*Xba*I sites of the pCS2+ vector. Alternatively, WT- or T2E-Rab37 were amplified by PCR using the primer sets (FP: 5′-ATATGCTACGTAGCCACCATGACGGGCGATTACAAGGATGACGACGATAAGACGCCAGGCGCCGTTGCC-3′ and RP: 5′-ATGCTAGTCGACTCACATGAAGGAGCAGCAGCT-3′) or (FP: 5′-ATATGCTACGTAGCCACCATGGAAGGCGATTACAAGGATGACGACGATAAGACGCCAGGCGCCGTTGCC-3′ and RP: 5′-ATGCTAGTCGACTCACATGAAGGAGCAGCAGCT-3′), respectively, and cloned into

the *Sna*BI/*Sal*I sites of the pBABE.puro retroviral vector. pCDNA5/FRT/WT-Rab37 was generated by PCR amplifying wildtype Rab37 using the primer set (FP: 5′-ATATGCGGATCCGCCACCATGACGGGCGATTACAAGGATGACGACGATAAGACGCCAGGCGCCGTTGCC-3′ and RP: 5′-ATGCTAGGGCCCTCACATGAAGGAGCAGCAGCT-3′) and cloned between the *Bam*H1/*Aga*1 sites of pCDNA5/FRT (Invitrogen). The Rab37-Q89L and -T43N mutants were generated using the Stratagene Quikchange Site-Directed Mutagenesis Kit (Agilent Technologies, Santa Clara, CA) from pCS2+/WT-Rab37 using the primer sets (FP: 5′-ACACCGCTGGGCTGGAACGGTTCCG-3′ and RP: 5′-CGGAACCGTTCCAGCCCAGCGGTGT-3′) or (FP: 5′-GAGACACAGGCGTCGGCAAAAATTGTTTCCTGATCCAATT-3′ and RP: 5′-AATTGGATCAGGAAACAATTTTTGCCGACGCCTGTGTCTC –3′), respectively. The pBABE.ble/HA-ΔDIX-Dvl2 vector was constructed as described previously (Zhang, et al., 2006). Membrane-localized mCherry and Centrin-GFP cloned into pCS2+ were obtained from S. Holley (Yale University).

N-terminal positional proteomics screen

MPE cells were cultured D-MEM-Flex media (Invitrogen) supplemented with (‘heavy’) [$^{13}C_6$]Arg or (‘light’) [$^{12}C_6$]Arg (100 mg/mL) for seven passages and then treated with TNP-470 (50 nM, 16 hr) or DMSO, respectively. Cells were resuspended in isotonic lysis buffer (25 mM Tris, pH 7.4) and lysed by passage through a Dounce homogenizer. Cell debris was removed by low-speed centrifugation (2,000 rpm, 5 min, 4 °C) followed by isolation of soluble fractions (S100) by high-speed centrifugation (42,000 rpm, 45 min, 4 °C). N-terminal peptides were enriched from S100 fractions and analyzed by LC-MS/MS as described previously (McDonald, et al., 2005).

Immunoblotting

Preparation of whole cell lysates and immunoblotting was conducted as described previously (Hines, et al., 2010). Antibodies detecting the FLAG epitope tag (cat #F1804) and β-actin (cat# A2228) were obtained from Sigma-Aldrich (St. Louis, MO), while the antibody for the HA epitope tag (cat# 3724) was purchased from Cell Signaling (Beverly, MA).

Immunofluorescence

Briefly, HEK 293T cultured on poly-L-lysine (100 μg/mL) coated glass coverslips were transfected with Rab37 constructs or RFP-Rab5 (cat# 14437, Addgene) using Lipofectamine 2000 (Invitrogen). HUVE cells were electroporated with the same constructs using the BTX electroporation kit (cat# 45-0803) and an ECM 830 electroporator machine (settings: 160V, 20 msec pulse) and then seeded on 0.8% gelatin-coated coverslips. Immunofluorescence staining and confocal microscopy was conducted as described previously (Cirone, et al., 2008). The antibody detecting Giantin (cat# ab24586) was obtained from Abcam (Cambridge, MA), the antibody against protein disulphide isomerase (cat# 2446) was from Cell Signaling and the antibody targeting GM130 (cat# 610822) was obtained from BD Biosciences.

[^{3}H]-thymidine incorporation

HEK 293T or HUVE cells were seeded into 96-well plates in growth media at a density of 3 $\times 10^3$ cells/well followed by TNP-470 treatments and assessment of [^{3}H]-thymidine incorporation as described previously (Hines, et al., 2010).

Endothelial cell network formation

Network formation assays were performed on Matrigel™ (BD Biosciences, San Jose, CA) basement membranes as described previously (Cirone, et al., 2008).

Zebrafish manipulation

Zebrafish (*Danio rerio*) embryos were collected from natural spawning. cDNA encoding WT-Rab37, T2E-Rab37, membrane-localized mCherry or Centrin-GFP cloned into the pCS2+ expression vector were linearized and synthetic RNAs were produced with the mMessage mMachine Capped RNA transcription kit (Ambion) using SP6 RNA polymerase. Zebrafish embryos were injected at one cell stage into the yolk with ~4–6 nL of 200 ng/μL of each RNA as described previously (Cirone, et al., 2008). Live embryos were photographed after orienting on 3% methylcellulose. A Zeiss Stereo Discovery.V12 microscope equipped with an AxioVision camera and software was used to acquire images. For neural tube morphology, live embryos at 28–30 hours post fertilization were oriented in low melt agarose and analyzed using a Leica SP2 laser confocal microscope system with 63× magnification and 2x zoom. Images are representative of maximum projections of six focal planes (z-series).

Statistical analysis

Data analysis was conducted using Prism v4.0b software (GraphPad Software Inc., San Diego, CA). Student's *t* test and one- or two-way ANOVA analysis were conducted as appropriate.

Supplementary Material

Refer to Web version on PubMed Central for supplementary material.

Acknowledgments

The authors acknowledge Dr. Taavi Neklesa and Dr. John Hines for helpful discussions and critical review of the manuscript. This work was supported by National Institutes of Health Grant CA083048 (to C.M.C) and CA112369 (to D.C.S) and a Biotechnology and Biological Sciences Research Council Grant (BB/F004699/1) to RJB. P.C. is a recipient of a Leukemia and Lymphoma Society Fellowship and T.B.S. is supported by an American Cancer Society Post-Doctoral Fellowship.

References

Angers S, Moon RT. Proximal events in Wnt signal transduction. Nat Rev Mol Cell Biol. 2009; 10:468–477. [PubMed: 19536106]

Arico-Muendel CC, Benjamin DR, Caiazzo TM, Centrella PA, Contonio BD, Cook CM, Doyle EG, Hannig G, Labenski MT, Searle LL, et al. Carbamate analogues of fumagillin as potent, targeted inhibitors of methionine aminopeptidase-2. J Med Chem. 2009; 52:8047–8056. [PubMed: 19929003]

Arnesen T, Van Damme P, Polevoda B, Helsens K, Evjenth R, Colaert N, Varhaug JE, Vandekerckhove J, Lillehaug JR, Sherman F, et al. Proteomics analyses reveal the evolutionary conservation and divergence of N-terminal acetyltransferases from yeast and humans. Proceedings of the National Academy of Sciences of the United States of America. 2009; 106:8157–8162. [PubMed: 19420222]

Borovina A, Superina S, Voskas D, Ciruna B. Vangl2 directs the posterior tilting and asymmetric localization of motile primary cilia. Nat Cell Biol. 2010; 12:407–412. [PubMed: 20305649]

Breuza L, Halbeisen R, Jeno P, Otte S, Barlowe C, Hong W, Hauri HP. Proteomics of endoplasmic reticulum-Golgi intermediate compartment (ERGIC) membranes from brefeldin A-treated HepG2 cells identifies ERGIC-32, a new cycling protein that interacts with human Erv46. J Biol Chem. 2004; 279:47242–47253. [PubMed: 15308636]

Brunner Y, Coute Y, Iezzi M, Foti M, Fukuda M, Hochstrasser DF, Wollheim CB, Sanchez JC. Proteomics analysis of insulin secretory granules. Mol Cell Proteomics. 2007; 6:1007–1017. [PubMed: 17317658]

Bucci C, Parton RG, Mather IH, Stunnenberg H, Simons K, Hoflack B, Zerial M. The small GTPase rab5 functions as a regulatory factor in the early endocytic pathway. Cell. 1992; 70:715–728. [PubMed: 1516130]

Carmeliet P. Angiogenesis in life, disease and medicine. Nature. 2005; 438:932–936. [PubMed: 16355210]

Cheng CW, Yeh JC, Fan TP, Smith SK, Charnock-Jones DS. Wnt5a-mediated non-canonical Wnt signalling regulates human endothelial cell proliferation and migration. Biochem Biophys Res Commun. 2008; 365:285–290. [PubMed: 17986384]

Cirone P, Lin S, Griesbach HL, Zhang Y, Slusarski DC, Crews CM. A role for planar cell polarity signaling in angiogenesis. Angiogenesis. 2008; 11:347–360. [PubMed: 18798004]

Folkman J. Angiogenesis: an organizing principle for drug discovery? Nat Rev Drug Discov. 2007; 6:273–286. [PubMed: 17396134]

Franch HA, Sooparb S, Du J, Brown NS. A mechanism regulating proteolysis of specific proteins during renal tubular cell growth. J Biol Chem. 2001; 276:19126–19131. [PubMed: 11262416]

Griffith EC, Su Z, Turk BE, Chen S, Chang YH, Wu Z, Biemann K, Liu JO. Methionine aminopeptidase (type 2) is the common target for angiogenesis inhibitors AGM-1470 and ovalicin. Chem Biol. 1997; 4:461–471. [PubMed: 9224570]

Grosshans BL, Ortiz D, Novick P. Rabs and their effectors: achieving specificity in membrane traffic. Proc Natl Acad Sci U S A. 2006; 103:11821–11827. [PubMed: 16882731]

Heisenberg CP, Tada M, Rauch GJ, Saude L, Concha ML, Geisler R, Stemple DL, Smith JC, Wilson SW. Silberblick/Wnt11 mediates convergent extension movements during zebrafish gastrulation. Nature. 2000; 405:76–81. [PubMed: 10811221]

Hines J, Ju R, Dutschman GE, Cheng YC, Crews CM. Reversal of TNP-470-induced endothelial cell growth arrest by guanine and guanine nucleosides. J Pharmacol Exp Ther. 2010; 334:729–738. [PubMed: 20571059]

Hwang CS, Shemorry A, Varshavsky A. N-Terminal Acetylation of Cellular Proteins Creates Specific Degradation Signals. Science. 2010; 327:973–977. [PubMed: 20110468]

Ingber D, Fujita T, Kishimoto S, Sudo K, Kanamaru T, Brem H, Folkman J. Synthetic analogues of fumagillin that inhibit angiogenesis and suppress tumour growth. Nature. 1990; 348:555–557. [PubMed: 1701033]

Ju R, Cirone P, Lin S, Griesbach H, Slusarski DC, Crews CM. Activation of the planar cell polarity formin DAAM1 leads to inhibition of endothelial cell proliferation, migration, and angiogenesis. Proc Natl Acad Sci U S A. 2010; 107:6906–6911. [PubMed: 20351293]

Kruger EA, Figg WD. TNP-470: an angiogenesis inhibitor in clinical development for cancer. Expert Opin Investig Drugs. 2000; 9:1383–1396.

Lee RH, Iioka H, Ohashi M, Iemura S, Natsume T, Kinoshita N. XRab40 and XCullin5 form a ubiquitin ligase complex essential for the noncanonical Wnt pathway. EMBO J. 2007; 26:3592–3606. [PubMed: 17627283]

Li X, Chang YH. Amino-terminal protein processing in Saccharomyces cerevisiae is an essential function that requires two distinct methionine aminopeptidases. Proc Natl Acad Sci U S A. 1995; 92:12357–12361. [PubMed: 8618900]

Marino JP Jr, Fisher PW, Hofmann GA, Kirkpatrick RB, Janson CA, Johnson RK, Ma C, Mattern M, Meek TD, Ryan MD, et al. Highly potent inhibitors of methionine aminopeptidase-2 based on a 1,2,4-triazole pharmacophore. J Med Chem. 2007; 50:3777–3785. [PubMed: 17636946]

Masckauchan TN, Agalliu D, Vorontchikhina M, Ahn A, Parmalee NL, Li CM, Khoo A, Tycko B, Brown AM, Kitajewski J. Wnt5a signaling induces proliferation and survival of endothelial cells in vitro and expression of MMP-1 and Tie-2. Mol Biol Cell. 2006; 17:5163–5172. [PubMed: 17035633]

Masuda ES, Luo Y, Young C, Shen M, Rossi AB, Huang BC, Yu S, Bennett MK, Payan DG, Scheller RH. Rab37 is a novel mast cell specific GTPase localized to secretory granules. FEBS Lett. 2000; 470:61–64. [PubMed: 10722846]

McDonald L, Robertson DH, Hurst JL, Beynon RJ. Positional proteomics: selective recovery and analysis of N-terminal proteolytic peptides. Nat Methods. 2005; 2:955–957. [PubMed: 16299481]

Mottola G, Classen AK, Gonzalez-Gaitan M, Eaton S, Zerial M. A novel function for the Rab5 effector Rabenosyn-5 in planar cell polarity. Development. 2010; 137:2353–2364. [PubMed: 20534670]

Pataki C, Matusek T, Kurucz E, Ando I, Jenny A, Mihaly J. Drosophila Rab23 is involved in the regulation of the number and planar polarization of the adult cuticular hairs. Genetics. 2010; 184:1051–1065. [PubMed: 20124028]

Pfeffer S, Aivazian D. Targeting Rab GTPases to distinct membrane compartments. Nat Rev Mol Cell Biol. 2004; 5:886–896. [PubMed: 15520808]

Piel M, Meyer P, Khodjakov A, Rieder CL, Bornens M. The respective contributions of the mother and daughter centrioles to centrosome activity and behavior in vertebrate cells. J Cell Biol. 2000; 149:317–330. [PubMed: 10769025]

Purvanov V, Koval A, Katanaev VL. A direct and functional interaction between Go and Rab5 during G protein-coupled receptor signaling. Sci Signal. 2010; 3:ra65. [PubMed: 20736485]

Rauch GJ, Hammerschmidt M, Blader P, Schauerte HE, Strahle U, Ingham PW, McMahon AP, Haffter P. Wnt5 is required for tail formation in the zebrafish embryo. Cold Spring Harb Symp Quant Biol. 1997; 62:227–234. [PubMed: 9598355]

Seifert JR, Mlodzik M. Frizzled/PCP signalling: a conserved mechanism regulating cell polarity and directed motility. Nat Rev Genet. 2007; 8:126–138. [PubMed: 17230199]

Sin N, Meng L, Wang MQ, Wen JJ, Bornmann WG, Crews CM. The anti-angiogenic agent fumagillin covalently binds and inhibits the methionine aminopeptidase, MetAP-2. Proc Natl Acad Sci U S A. 1997; 94:6099–6103. [PubMed: 9177176]

Staton CA, Stribbling SM, Tazzyman S, Hughes R, Brown NJ, Lewis CE. Current methods for assaying angiogenesis in vitro and in vivo. Int J Exp Pathol. 2004; 85:233–248. [PubMed: 15379956]

Stenmark H. Rab GTPases as coordinators of vesicle traffic. Nat Rev Mol Cell Biol. 2009; 10:513–525. [PubMed: 19603039]

Tada M, Smith JC. Xwnt11 is a target of Xenopus Brachyury: regulation of gastrulation movements via Dishevelled, but not through the canonical Wnt pathway. Development. 2000; 127:2227–2238. [PubMed: 10769246]

Turk BE, Griffith EC, Wolf S, Biemann K, Chang YH, Liu JO. Selective inhibition of amino-terminal methionine processing by TNP-470 and ovalicin in endothelial cells. Chem Biol. 1999; 6:823–833. [PubMed: 10574784]

Wall DS, Gendron RL, Good WV, Miskiewicz E, Woodland M, Leblanc K, Paradis H. Conditional knockdown of tubedown-1 in endothelial cells leads to neovascular retinopathy. Investigative Ophthalmology & Visual Science. 2004; 45:3704–3712. [PubMed: 15452080]

Wallingford JB, Habas R. The developmental biology of Dishevelled: an enigmatic protein governing cell fate and cell polarity. Development. 2005; 132:4421–4436. [PubMed: 16192308]

Wallingford JB, Rowning BA, Vogeli KM, Rothbacher U, Fraser SE, Harland RM. Dishevelled controls cell polarity during Xenopus gastrulation. Nature. 2000; 405:81–85. [PubMed: 10811222]

Wang GT, Mantei RA, Kawai M, Tedrow JS, Barnes DM, Wang J, Zhang Q, Lou P, Garcia LA, Bouska J, et al. Lead optimization of methionine aminopeptidase-2 (MetAP2) inhibitors containing sulfonamides of 5,6-disubstituted anthranilic acids. Bioorg Med Chem Lett. 2007; 17:2817–2822. [PubMed: 17350258]

Wang J, Tucker LA, Stavropoulos J, Zhang Q, Wang YC, Bukofzer G, Niquette A, Meulbroek JA, Barnes DM, Shen J, et al. Correlation of tumor growth suppression and methionine aminopetidase-2 activity blockade using an orally active inhibitor. Proc Natl Acad Sci U S A. 2008; 105:1838–1843. [PubMed: 18252827]

Warder SE, Tucker LA, McLoughlin SM, Strelitzer TJ, Meuth JL, Zhang Q, Sheppard GS, Richardson PL, Lesniewski R, Davidsen SK, et al. Discovery, identification, and characterization of candidate pharmacodynamic markers of methionine aminopeptidase-2 inhibition. J Proteome Res. 2008; 7:4807–4820. [PubMed: 18828628]

Xiao Q, Zhang F, Nacev BA, Liu JO, Pei D. Protein N-terminal processing: substrate specificity of Escherichia coli and human methionine aminopeptidases. Biochemistry. 2010; 49:5588–5599. [PubMed: 20521764]

Xiao Q, Zhang FR, Nacev BA, Liu JO, Pei DH. Protein N-Terminal Processing: Substrate Specificity of Escherichia coli and Human Methionine Aminopeptidases. Biochemistry. 2010; 49:5588–5599. [PubMed: 20521764]

Ye X, Wang Y, Cahill H, Yu M, Badea TC, Smallwood PM, Peachey NS, Nathans J. Norrin, frizzled-4, and Lrp5 signaling in endothelial cells controls a genetic program for retinal vascularization. Cell. 2009; 139:285–298. [PubMed: 19837032]

Yeh JR, Ju R, Brdlik CM, Zhang W, Zhang Y, Matyskiela ME, Shotwell JD, Crews CM. Targeted gene disruption of methionine aminopeptidase 2 results in an embryonic gastrulation defect and endothelial cell growth arrest. Proc Natl Acad Sci U S A. 2006; 103:10379–10384. [PubMed: 16790550]

Zhang Y, Yeh JR, Mara A, Ju R, Hines JF, Cirone P, Griesbach HL, Schneider I, Slusarski DC, Holley SA, et al. A chemical and genetic approach to the mode of action of fumagillin. Chem Biol. 2006; 13:1001–1009. [PubMed: 16984890]

HIGHLIGHTS

- N-terminal positional proteomics identifies Rab37 as a novel MetAP-2 substrate.
- Rab37 appears to play a role in plasma membrane to Golgi trafficking.
- Aberrant Rab37 accumulation disrupts normal endothelial cell function.
- Rab37 expression perturbs Wnt PCP-dependent process during zebrafish development.

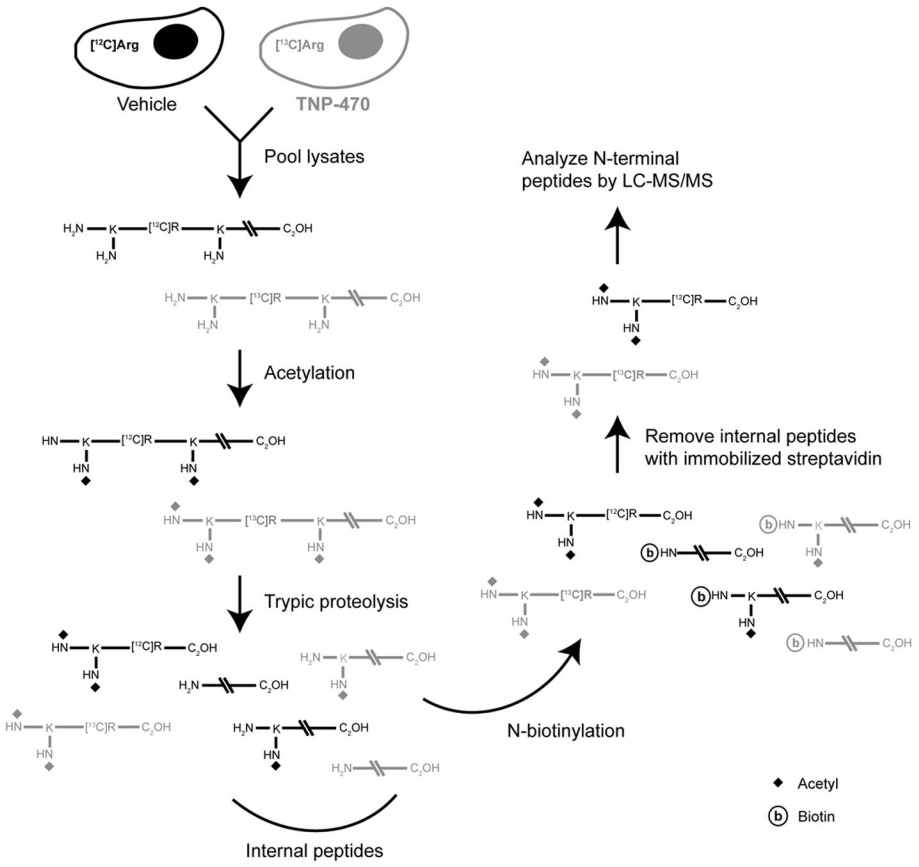

Figure 1. Identification of MetAP-2 substrates by N-terminal positional proteomics

MPE cells cultured in media containing stable heavy isotope-labeled arginine ([$^{13}C_6$]Arg) were treated with TNP-470, while vehicle-treated cells were maintained in the presence of [$^{12}C_6$]Arg. Following cell lysis, soluble fractions from the two treatment conditions were pooled and N-terminal peptides isolated by the following reaction sequence: 1) proteomic chemical acetylation of primary amines on N-termini and lysine residue side chains, 2) tryptic proteolysis to generate blocked N-terminal peptides and internal peptides with newly exposed reactive α-amino groups, and 3) removal of these internal peptides by reaction with an immobilized amine capture reagent. Isolated N-terminal peptides can then be identified by LC-MS/MS and the role of MetAP-2 in N-terminal Met excision determined by comparing abundance of the ‘heavy’ (TNP-470-treated) versus ‘light’ (vehicle-treated) peptides.

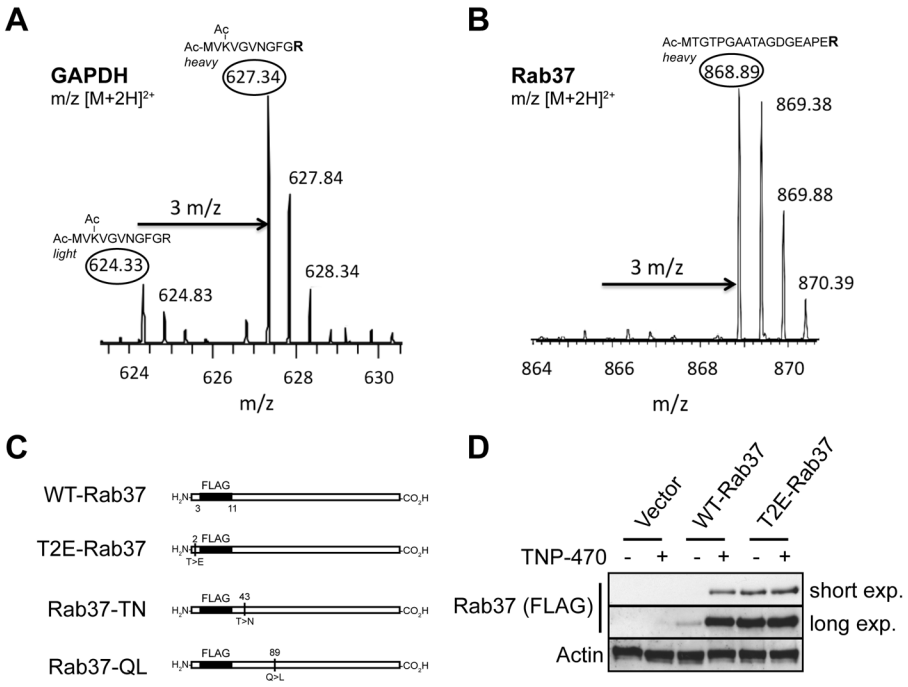

Figure 2. Rab37 is a novel MetAP-2 substrate

(*A* and *B*) LC-MS analysis of N-terminal peptides from MPE cells differentially labeled with [$^{13}C_6$]Arg before treatment with vehicle or TNP-470 (50 nM, 16 hr). Unprocessed N-terminal tryptic peptides are highlighted in the ovals. Note the peak height difference in the light, vehicle-treated and heavy (i.e., [$^{13}C_6$]Arg labeled) TNP-470 treated peptides for the known MetAP-2 substrate GAPDH. No light, vehicle-treated N-terminal trypic peptide was detected for the novel MetAP-2 substrate Rab37, suggesting that this protein is destabilized by NME. (*C*) Diagram of Rab37 constructs used in this study. (*D*) Whole cell lysates from HEK 293T cells transiently transfected with WT- or T2E-Rab37 (50 ng) or empty vector followed by incubation with vehicle or TNP-470 (50 nM, 16 hr) were immunoblotted with specific antibodies as indicated.

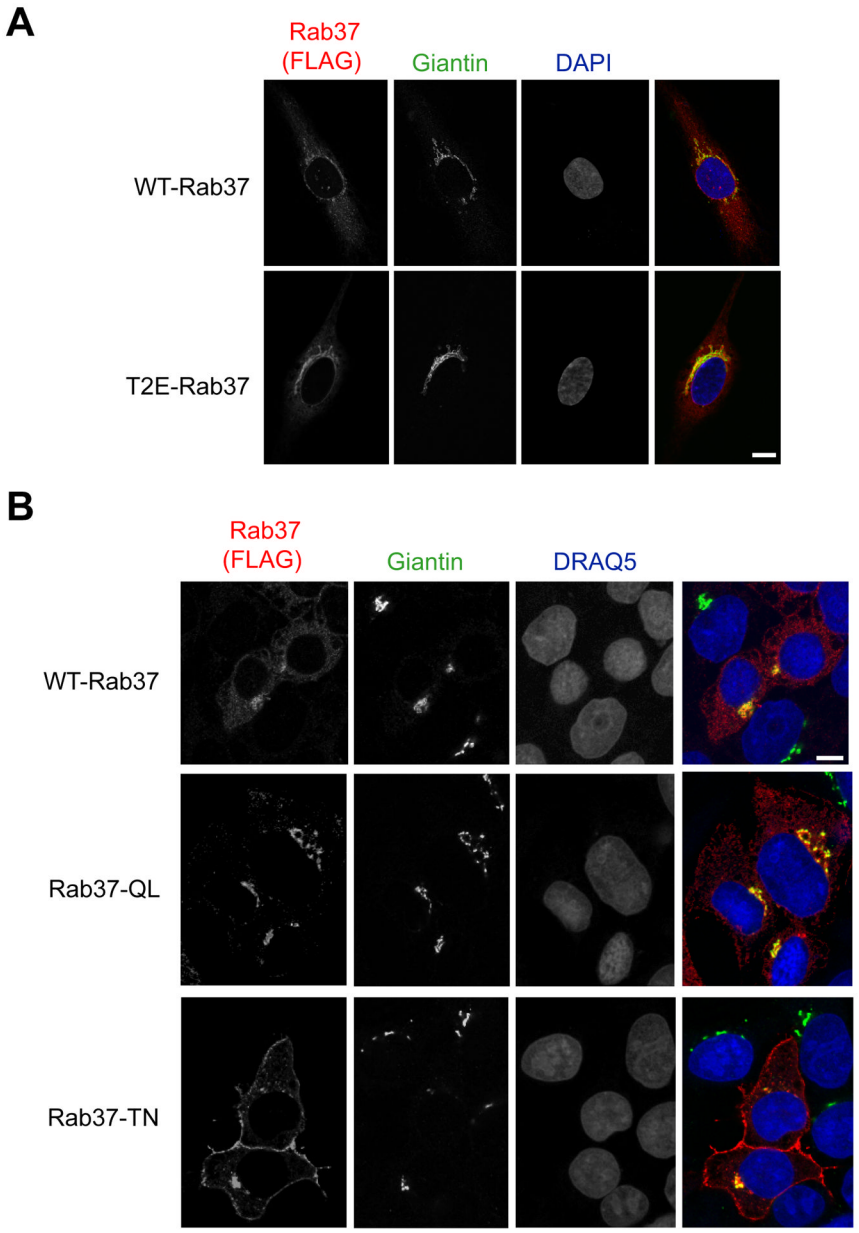

Figure 3. Localization of Rab37 GTPase cycle mutants suggests a role in plasma membrane to Golgi trafficking

(*A*) HUVE cells electroporated with WT- or T2E-Rab37 were cultured on gelatin-coated slides followed by staining with antibodies for FLAG and the Golgi marker Giantin. (*B*) HEK 293T cells transiently transfected with WT-Rab37, Rab37-Q89L or Rab37-T43N were cultured on poly-L-lysine coated slides followed by staining with antibodies specific for FLAG and the Golgi marker Giantin. *Scale bar*, 10 μm. See also Figures S1–S3.

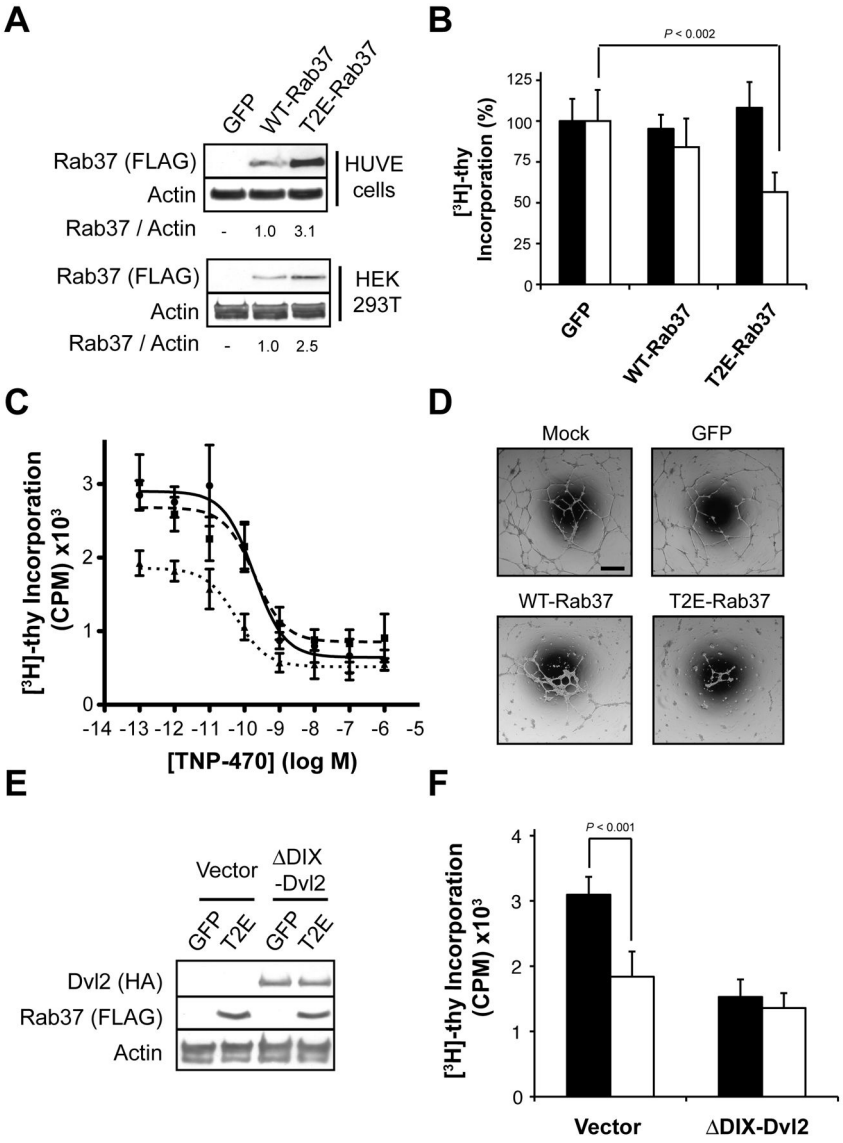

Figure 4. Aberrant Rab37 accumulation disrupts endothelial cell function

(*A*) Whole cell lysates from HUVE or HEK 293T cells stably expressing GFP or WT- or T2E-Rab37 were immunoblotted with specific antibodies as indicated. (*B*) Effect of stably expressing GFP or WT- or T2E-Rab37 on [^{3}H]-thymidine incorporation in HEK 293T cells (*black bars*) or HUVE cells (*white bars*). (*C*) HUVE cells stably expressing GFP (●, *solid line*), WT-Rab37 (■, *dashed line*) or T2E-Rab37 (▲, *dotted line*) were treated with the indicated concentrations of TNP-470 for 20 hr followed by labeling with [^{3}H]-thymidine (20 μCi/mL; 4 hr) before harvesting of nuclei. (*D*) Stable retroviral infection with WT- or T2E-Rab37 suppresses network formation in HUVE cells plated on Matrigel™ relative to cells stably infected with GFP or mock infected cells. *Scale bar*, 100 μm. (*E*) Whole cell lysates from HUVE cells stably expressing HA-ΔDIX-Dvl2 along with GFP or T2E-Rab37 were immunoblotted with specific antibodies as indicated. (*F*) Effect of stably expressing GFP (*black bars*) T2E-Rab37 (*white bars*) on [^{3}H]-thymidine incorporation in HUVE cells previously infected with HA-ΔDIX-Dvl2 or the corresponding vector control. See also Figure S4.

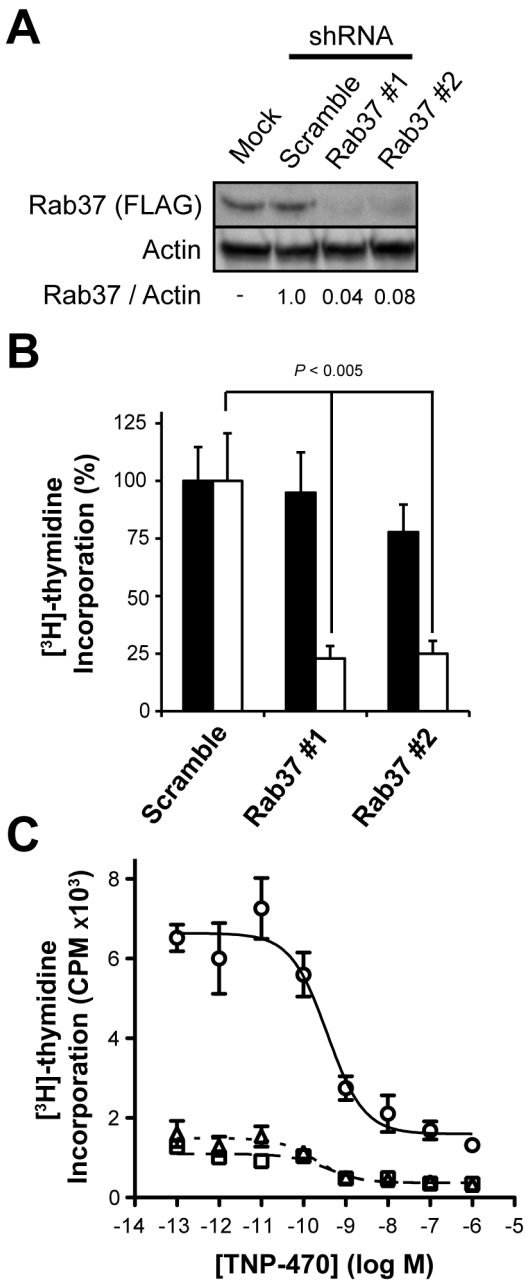

Figure 5. Rab37 is essential for endothelial cell proliferation

(*A*) Infecting HEK 293 cells stably expressing WT-Rab37 with lentiviral shRNA constructs targeting Rab37 reduced levels of this protein relative to a non-targeting scramble shRNA as detected by immunoblotting with specific antibodies as indicated. (*B*) Effect of stably expressing lentiviral shRNA constructs targeting Rab37 on [^{3}H]-thymidine incorporation in HEK 293 cells (*black bars*) or HUVE cells (*white bars*) versus a non-targeting scramble shRNA. (*C*) HUVE cells stably expressing Rab37 targeting shRNA #1 (△, *dotted line*) or #2 (□, *dashed line*) or a non-targeting scramble shRNA (○, *solid line*) were treated with the indicated concentrations of TNP-470 for 20 hr followed by labeling with [^{3}H]-thymidine (20 μCi/mL; 4 hr) and harvesting of nuclei.

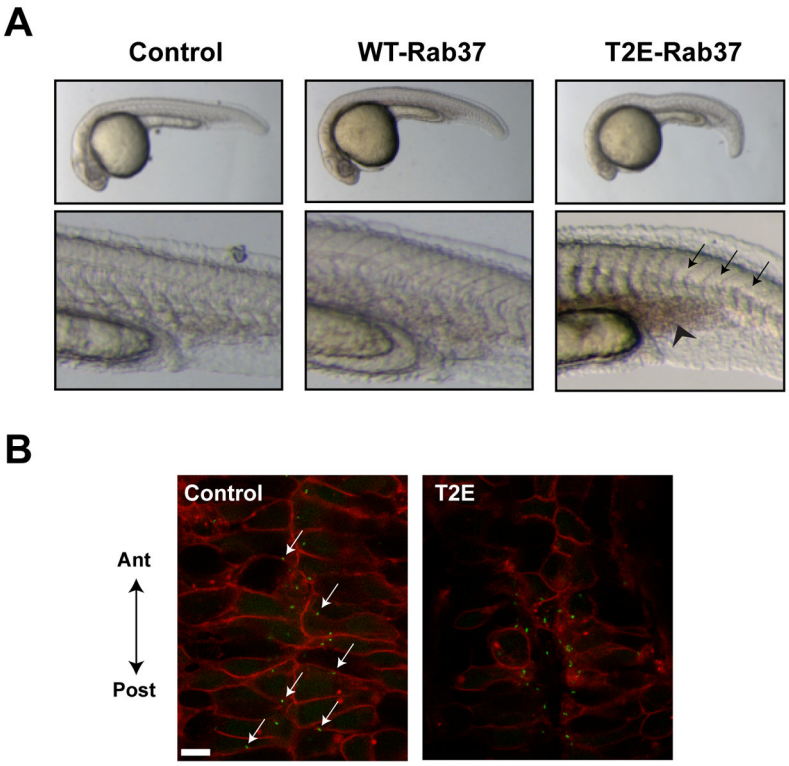

Figure 6. Rab37 expression phenocopies loss of Wnt PCP signaling during zebrafish development

(*A*) Uninjected (*Control*) zebrafish embryos 24 hr post-fertilization display a straight notochord characterized by the presence of 'chevron-shaped' somites. Injection with wildtype Rab37 RNA results in slight shortening of the anterior-posterior axis, while embryos injected with T2E-Rab37 RNA results in notochord undulations and formation of "C-shaped" somites (*black arrows*) leading to severe shortening and kinking of the anterior-posterior axis. Additionally, embryos injected with T2E-Rab37 RNA display an accumulation of blood posterior to the yolk extension (*black chevron*), which suggests impaired vasculogenesis. (*B*) Confocal images of the neural floorplate of zebrafish embryos injected with membrane-localized mCherry and Centrin-GFP in the presence/absence of T2E-Rab37. Centrin-GFP is localized to the posterior membrane of control-injected embryos (*white arrows*), while overall morphogenesis and centrin localization is disrupted in embryos injected with T2E-Rab37 RNA.

Table 1

Quantification of developmental defects caused by aberrant Rab37 expression during zebrafish embryogenesis.

RNA	Wildtype-like	C-shaped somites	Undulated notochord	% Morphant
Control	77	-	1	1%
WT-Rab37	100	8	5	11%
T2E-Rab37	95	20	14	26%